

# Temporal Coding in Neuronal Populations in the Presence of Axonal and Dendritic Conduction Time Delays

David M. Halliday

Department of Electronics, University of York, Heslington, YORK, YO10 5DD, UK.  
[dh20@ohm.york.ac.uk](mailto:dh20@ohm.york.ac.uk)

**Abstract.** Time delays are a ubiquitous feature of neuronal systems. Synaptic integration between spiking neurones is subject to time delays at the axonal and dendritic level. Recent evidence suggests that temporal coding on a millisecond time scale may be an important functional mechanism for synaptic integration. This study uses biophysical neurone models to examine the influence of dendritic and axonal conduction time delays on the sensitivity of a neurone to temporal coding in populations of synaptic inputs. The results suggest that these delays do not affect the sensitivity of a neurone to the presence of temporal correlation amongst input spike trains, and point to a mechanism other than electrotonic conduction of EPSPs to describe neural integration under conditions of large scale synaptic input. The results also suggest that it is the common modulation rather than the synchronous aspect of temporal coding in the input spike trains which neurones are sensitive to.

## 1. Introduction

Recent experimental evidence has emerged that temporal coding on a millisecond time scale may underlie the representation and transmission of information between neurones within the central nervous system [1,2,3]. Modelling studies have highlighted both rate coding and temporal coding as candidate mechanisms which may subserve neural integration between populations of spiking neurones [4-10].

An important aspect of neuronal systems is the presence of both axonal and dendritic conduction time delays. This study investigates whether these delays impact on temporal coding in neurones, by determining if they alter the ability of a neurone to respond to temporal coding in pre-synaptic inputs. In this study, temporal coding is carried as temporal correlation amongst a population of input spike trains. We consider a realistic correlation structure amongst the spike trains in the population. This correlation is both weak and stochastic, and is based on common rhythmic modulation of spike trains, which induces a tendency for synchronised firing. The resultant temporal correlation is manifest as a rhythmic modulation of inter spike intervals in individual spike trains and a tendency for synchronised firing between sample pairs of spike trains [11].

This paper addresses the question of propagation of temporal coding within neurones under conditions of large scale synaptic input, and in particular how temporal coding on a millisecond time scale can be achieved in the presence of

dendritic and axonal conduction delays of a similar order of magnitude. We use simulations of biophysical neurone models, based on a compartmental model to study how the spatial and temporal aspects of large scale synaptic input interact and shape the output discharge. The simulations are based on a class of neurones which have been extensively studied and possess dendritic trees which have electrotonic conduction time delays of the order of several milliseconds, spinal motoneurons. The simulations capture the large degree of convergence present in neural systems, where each neurone is acted on by a large number of inputs which are distributed over the surface area of the dendritic tree and cell body.

The results of the simulations show that, under conditions of large scale synaptic input, temporal coding can be preserved in the output discharge when the temporal code is carried by a subset of the total synaptic input in the form of temporally correlated spike trains. Dendritic conduction time delays do not affect this process, similar results are obtained with temporally correlated inputs which have a high degree of spatial correlation (clustered) or a low degree of spatial correlation (distributed). The inclusion of random axonal conduction delays similarly does not alter the results. This suggests that a mechanism other than electrotonic conduction of EPSPs is responsible for synaptic integration and the propagation of temporal coding under conditions of large scale synaptic input.

## 2. Model Neurone

The model motoneurone is based on morphological studies of cat spinal  $\alpha$  motoneurons [12] and consists of a spherical soma from which radiate 12 tapered dendrites of different lengths. These 12 dendrites consist of three types, which we call short, medium and long, each cell contains four of each type. The membrane parameters are based on complementary electrophysiological studies of the same motoneurons [13,14], these are a membrane resistivity,  $R_m$ , of  $11,000 \Omega\text{-cm}^2$ , a cytoplasmic resistivity,  $R_i$ , of  $70 \Omega\text{-cm}$ , and a membrane capacitance,  $C_m$ , of  $1.0 \mu\text{F}/\text{cm}^2$ . The initial diameters at the soma of the three dendrite types are  $5.0 \mu\text{m}$  (short),  $7.5 \mu\text{m}$  (medium) and  $10.0 \mu\text{m}$  (long). The taper used to estimate dendritic diameters is  $0.5 \mu\text{m}$  reduction per  $100 \mu\text{m}$  length. The physical lengths of the three dendrite types are  $766 \mu\text{m}$  (short),  $1258 \mu\text{m}$  (medium) and  $1904 \mu\text{m}$  (long), the equivalent passive electrotonic lengths are  $L=0.7$ ,  $1.0$  and  $1.5$ , respectively. The dendritic tree and soma are modelled using a compartmental model [15], with the dendrites represented as a sequence of connected cylinders, each of electrotonic length  $L=0.1$ , with an additional compartment for the soma. Thus a total of 129 compartments are used to model each motoneurone. The total membrane areas represented in the compartmental model for each dendrite type are  $8100 \mu\text{m}^2$  (short),  $18500 \mu\text{m}^2$  (medium) and  $33500 \mu\text{m}^2$  (long). The compartmental model for the complete cell represents a total membrane area of  $248300 \mu\text{m}^2$ , 97% of this area is taken up by the 12 dendrites. The model has a steady state input resistance of  $4.92 \text{M}\Omega$ , and a time constant of  $9.7 \text{ms}$ , estimated from the response to hyperpolarizing current injected at the soma.

Individual excitatory synaptic inputs use a time dependent conductance change, specified by an alpha function:  $g_{\text{syn}}(t) = G_s \frac{t}{\tau} \exp(-t/\tau)$  [16,17], where  $\tau$  is the time constant, and  $G_s$  a scaling factor which defines the peak conductance change. In the present study we use values of  $\tau = 0.2$  ms, and  $G_s = 1.19 \times 10^{-8}$  S, this results in a peak conductance change of 4.38 nS at  $t = 0.2$  ms [17]. A value of  $-70$  mV is used for the membrane resting potential, and the reversal potential for excitatory post synaptic potentials (EPSPs) is  $-10$  mV. This conductance change, when activated from the resting potential at the soma, results in an EPSP with a peak magnitude at the soma of  $100 \mu\text{V}$  at  $t = 0.525$  ms, and a rise time (10% to 90%) and half-width of 0.275 ms, 2.475 ms [18]. The time course of this EPSP is illustrated in Fig. 1 (top trace), as is the time course of the EPSP which is generated at the soma when the same conductance change is activated in the most distal compartments of each of the three dendrite types. The magnitudes of these EPSPs are  $52.8 \mu\text{V}$  (short dendrite),  $40.4 \mu\text{V}$  (medium) and  $27.1 \mu\text{V}$  (long). The delays to the peak of voltage response are 2.0 ms, 3.08 ms and 4.75 ms, the rise times are 0.90 ms, 1.35 ms and 2.08 ms, and the half widths are 7.05 ms, 9.35 ms and 11.38 ms, respectively. Comparison of the four traces in Fig. 1 illustrates the reduction in magnitude and increased conduction times associated with electrotonic conduction of localised voltage changes in passive dendrites. The resultant EPSPs generated at the soma are reduced in magnitude and spread out in time, reflecting the low pass filtering characteristics of dendrites [19].

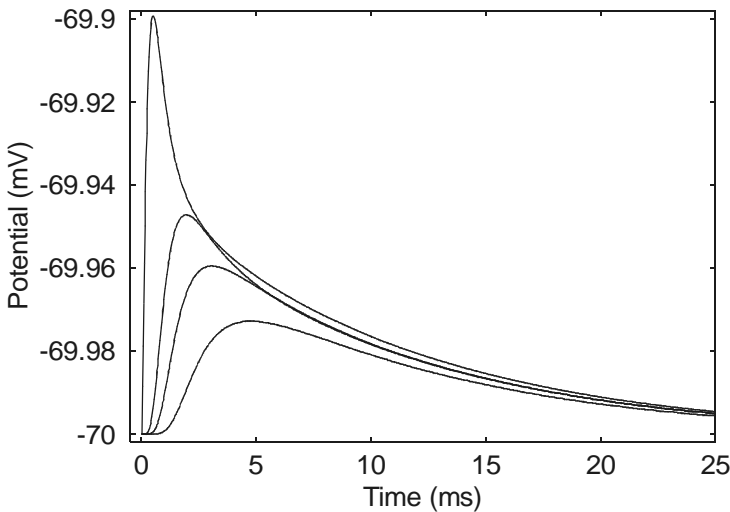


**Fig. 1.** Voltage response at soma to individual synaptic events activated at the soma (top trace) and in the most distal compartments of the short, medium and long (bottom trace) dendrite. These responses show a decreasing magnitude and increased time to peak voltage, effects due to electrotonic conduction in passive dendrites.

The threshold parameters and afterhyperpolarization (AHP) conductances associated with repetitive firing are based on the work of [20]. The firing threshold is  $-55$  mV, 15 mV above resting potential, [20] proposes a three term model for a time

dependent potassium conductance,  $g_k(t)$ . In the present study, we incorporate only the dominant F2 term (see [20]) in the AHP conductance model,  $g_k(t) = G_k \exp(-t/\tau_k)$ , with  $G_k = 6.0 \times 10^{-7}$  S, and  $\tau_k = 14$  ms. The reversal potential for this potassium conductance is  $-75$  mV. The other fast acting terms in the AHP conductance model [20] have no influence at the low firing rates in the present study, and are omitted. The AHP trajectory during repetitive firing at 12 spikes/sec, induced by constant current input to the soma, has a peak depression of 12 mV. An action potential is taken to occur when the somatic membrane potential exceeds the threshold, and  $g_k(t)$  is activated in the somatic compartment to simulate the AHP.

The results in figure 1 illustrate the dendritic conduction delays present in the model, these can be up to several milliseconds for more distal inputs to the dendritic tree. Thus, the spatial dimension converts to a temporal delay before the effects of synaptic input arrive at the soma by electrotonic conduction. The traces in Fig. 1 suggest that electrotonic conduction of EPSPs is the underlying mechanism by which sparse synaptic input to a dendritic tree acts to modulate the output discharge. The objective of this study is to assess if these time delays impact on the sensitivity of the neurone to temporal patterns in the timing of synaptic inputs under conditions of large scale synaptic input.

### 3. Assessing Temporal Coding in Neuronal Discharges

The approach we use to assess the presence of temporal coding in the output discharge of the neurone is the common input model [21]. In this approach, the total synaptic input to each cell is divided into common and independent components. The common component is shared by the two cells, and the inputs have identical input locations on both cells. A correlation analysis of the output discharge of two identical neurones models is used to infer what characteristics of the common input to the two cells have been preserved in the two output discharges. This analysis can detect the presence of temporal correlation between the output discharges, which is induced entirely by the common synaptic inputs. Such temporal correlation between the two output discharges indicates that the temporal code in the common inputs has been transmitted to the output discharge of the two neurones. The reasons for adopting this approach are twofold. The method is independent of the number of common inputs. This is in contrast to an input/output analysis for a single neurone which would depend on the number of inputs considered, and is not practical for the numbers of common inputs used in the present study (around 200). Experimentally the analysis of synchronised activity in ensembles of neurones is often based around detecting synchronized activity in macroscopic measures such as local field potential recordings. The common input simulation approach is closer to the experimental situation, where access to input signals are rarely possible in vivo.

We use the frequency domain analogue of time domain correlation, coherence functions [22, 23], to assess the temporal correlation between the output discharges of the paired neurone model. This has some advantages over a time domain approach, in particular the estimated coherence between the two output discharges can be used to directly infer the frequency content of the common inputs to the two cells [24], and thus indicates what frequency components in the temporal code are transmitted to the

output discharge of the neurones. Details of the derivation, estimation and interpretation of coherence functions can be found in the above references. Briefly, coherence functions provide a normative measure of linear association between two stationary stochastic signals (spike trains or time series data) on a scale from 0 to 1. Zero (more correctly values below a confidence limit) indicates no correlation between the signals, one indicates a perfect linear association. A coherence value is estimated for each frequency of interest over a range of frequencies, usually the Fourier frequencies resulting from the use of an FFT algorithm to calculate the discrete Fourier transform of the data. A confidence limit can be set based on the null hypothesis of independent signals, values of coherence below this can be taken as evidence of uncorrelated signals at a particular frequency. The model for interpreting coherence estimates between the output discharge of two neurones acted on by common synaptic input is described in [24]. The estimated coherence can be shown to be proportional to the spectrum of the common input signal for a single common input. We use this interpretation as the basis to interpret the result from the present simulations. Coherence is used to infer which frequency components in the common synaptic inputs are effective in modulating the output discharge of the two cells, providing an indication of preserved temporal coding in the two output discharges.

## 4. Results

The aim of this study is to investigate spatial temporal interactions in a dendritic structure, in other words how spatial and temporal correlations amongst a subset to the total synaptic input interact to shape the output discharge of the neurone. Spatial correlation refers to clustering of inputs about a particular location on the dendritic tree, measured as the passive electrotonic length from the soma. Temporal correlation refers to the correlation structure present in the population of input spike trains, measured as correlation between two sample input spike trains. The pre-synaptic inputs are distributed over the soma and all dendrites uniformly by surface area. The number of pre-synaptic inputs and the mean firing rate of each input spike train are adjusted such that each compartment receives the same average number of EPSP's/sec in all simulations. In the basic configuration each cell has a total of 996 inputs, 32 at the soma and 33, 74 and 134 inputs to each short, medium and long dendrite, with inputs distributed over all dendritic cylinders. The desired output rate for repetitive firing was chosen as 12 spikes/sec, to achieve this requires a total synaptic input of 31,872 EPSPs/sec, this can be achieved with each of the 996 inputs activated by a random (Poisson) spike train firing at 32 spikes/sec. During repetitive firing the membrane potential is dominated by the large AHP, approximately 12 mV in amplitude, following each output spike. Smaller fluctuations, approximately 1 mV peak-to-peak amplitude, are superimposed on top of this trajectory. These fluctuations are a result of spatial temporal interactions amongst the synaptic inputs, and are larger in magnitude than individual EPSPs [25]. It is these fluctuations and the process by which they modulate the output discharge which this study is concerned with.

Only the common subset of the total synaptic carries the temporal coding which is considered to provide the input "signal" to the two cells. In this study, the temporal coding is carried by two sets of synaptic inputs, each of which consist of 5% of the total synaptic input, measured as EPSPs/sec input to each neurone. These two

populations consist of 160 spike trains firing at 10 spikes/s and 64 spike trains firing at 25 spikes/s. These inputs are periodic and have a coefficient of variation (c.o.v.) of 0.1. Each population of spike trains has a weak stochastic correlation structure. The spike timings are generated by a population of integrate-and-fire encoders, with mean rates of 10 spikes/s or 25 spikes/s, respectively, within each population. Correlated spike times are generated by applying common pulse inputs to each population of encoders, these pulses are derived from a single spike train of rate 10 or 25 spikes/sec and a c.o.v. of 0.1. This approach generates spike trains which have a weak stochastic correlation structure between pairs of discharges, the aim is to model accurately the pattern of correlation found in mammalian central nervous systems. The strength of correlation within the two populations can be quantified using coherence analysis, for the present study the coherence between sample pairs of spike trains from each population is 0.015 at 10 Hz or 25 Hz, respectively. For details see [11]. This weak stochastic correlation links the timing of individual spikes across the two population of discharges to a single “parent” discharge of 10 spikes/s or 25 spike/s which is the source of the temporal coding in each population. The time course of the temporal correlation between inputs is a few ms (not shown). Thus, temporal coding is carried by a tendency for synchronized spikes occurring within a few ms.

The coherence results in this study are based on analysis of simulated output spike trains of duration 100 seconds with spike timings defined to an accuracy of 1 ms. The Fourier frequencies have a spacing of 0.977 Hz, this results from using a discrete Fourier transform length of 1024 points to construct spectra and coherence estimates.

Fig. 2 shows coherence estimates between the output discharges of the two model neurones with the two populations of common inputs applied in different input locations. The numbers of independent inputs and their activation rate are adjusted in each simulation so that each compartment receives the same average number of EPSPs/sec as the control configuration above. A Poisson discharge is used to activate all independent inputs to the two cells. Fig. 2a is a control case, when two populations of uncorrelated spike trains are applied as common input. These have the same firing rate and c.o.v. as the correlated spike trains, except there is no temporal correlation between the spike times within each population, and thus no temporal code. Figures 2b, 2c and 2d show the effects of applying the correlated spike train inputs with a high degree of spatial correlation (clustering) at different electrotonic lengths from the soma, concentrated around  $L=0.0$  to  $0.1$  (Fig. 2b),  $L=0.5$  to  $0.6$  (Fig. 2c) and  $L=0.8$  to  $1.1$  (Fig. 2d). This last case has no common inputs to the 4 short dendrites, which have a passive electrotonic length of  $0.7$ . Fig. 3a shows the estimated coherence between the two output discharges with the common correlated inputs uniformly distributed over the entire dendritic tree, this represents the smallest spatial correlation amongst input locations.

The coherence estimates in Fig. 2b, 2c, 2d and 3a are similar in form. Both have distinct peaks at 10 Hz and 25 Hz, indicating that the output discharges of the two model neurones are correlated only at the frequencies at which the two populations of common inputs are correlated. This correlation does not reflect the firing rates of the two populations of input spike times, since the coherence estimate for the simulation with uncorrelated periodic inputs at 10 and 25 spikes/sec is not significant (Fig. 2a). The strength of correlation between the two output discharges is an order of magnitude larger than the strength of correlation amongst the two populations of correlated inputs (see above). We interpret the coherence between the two output discharges to indicate that the temporal coding in each population of correlated input

spike trains is preserved in the output discharges of the two neurones. These results suggest that the location of the synaptic inputs on the dendritic tree does not influence the sensitivity of the neurone to the presence of temporal coding in the common synaptic inputs.

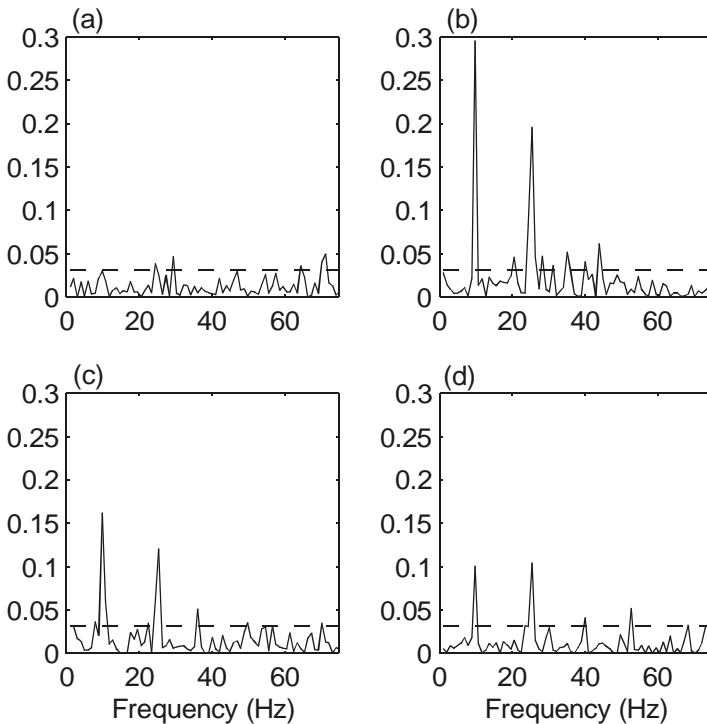


**Fig. 2.** Coherence estimate between the output discharges of the two cell model with (a) two populations of uncorrelated spike train input applied to  $L=0.0, 0.1$ , and two populations of weakly correlated spike trains applied to (b)  $L=0.0, 0.1$ , (c)  $L=0.5, 0.6$  and (d)  $L=0.8$  to  $1.1$ . For both the correlated and uncorrelated inputs, each population constitutes 5% of the total synaptic input (160 inputs at 10 spikes/sec and 64 inputs at 25 spikes/sec). The dashed horizontal lines are upper 95% confidence limits based on the assumption of independence. Coherence estimates constructed from 100 seconds of simulated data.

We next consider the effect of adding an axonal conduction delay to the configuration with uniformly distributed common inputs (Fig. 3a). In Fig. 3b is a coherence estimate between the two output discharges with the addition of a fixed, randomly chosen, delay to both branches of each common synaptic input. The delay was normally distributed with a value of  $2.5 \pm 2.3$  ms (mean  $\pm 2$  SD). This coherence estimate still has distinct peaks at 10 Hz and 25 Hz, indicating that the random axonal delay also has a minimal effect on the sensitivity of the neurones to the temporal correlation amongst the populations of common input spike trains.

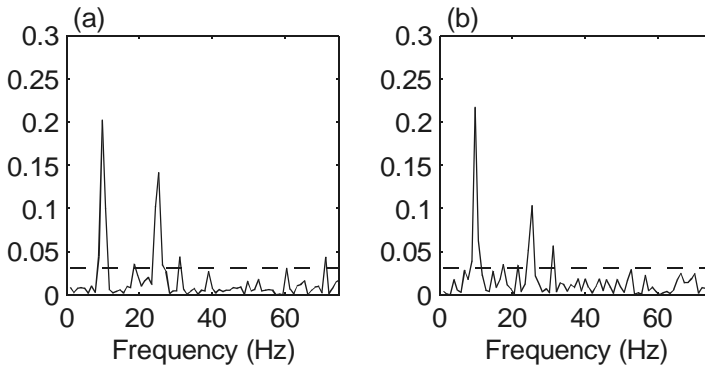


**Fig. 3.** Coherence estimate with two populations of weakly correlated spike trains applied uniformly by membrane surface area over the dendritic tree, (a) without any axonal conduction delay, and (b) including a fixed, randomly chosen, axonal conduction delay to each synaptic input. Each population of inputs constitutes 5% of the total synaptic input (160 inputs at 10 spikes/sec and 64 inputs at 25 spikes/sec). The dashed horizontal lines are upper 95% confidence limits based on the assumption of independence. Coherence estimates constructed from 100 seconds of simulated data.

## 5. Discussion

The above results suggest that synaptic input location has little effect on the ability of the neurone to detect the presence of temporal correlation in populations of synaptic inputs (Fig. 2b, 2c, 2d, 3). In contrast, populations of synaptic input with the same rhythmic components, but which are uncorrelated, have no significant effect on the output discharge (Fig. 2a). The results are obtained despite the considerable electrotonic conduction time delay present for the effects of individual synaptic inputs to propagate to the somatic spike generation site, which are the order of several ms (Fig. 1). This time delay is similar to the time course of the temporal correlation amongst inputs. In light of these results it seems reasonable to suggest that a mechanism other than electrotonic conduction of EPSPs is the dominant mechanism whereby temporal coding amongst input spike trains modulates the output discharge of each neurone.

The temporal code in this study is carried by rhythmic components which result in weak stochastic temporal correlation between pairs of spike trains within the population of inputs. In the temporal domain this is manifest as a tendency for synchronous discharge. An interesting question is whether it is the tendency for synchronous discharge within a time scale of a few ms, or the presence of common rhythmic modulation which the neurone is sensitive to. The inclusion of a random axonal conduction delay prior to the activation of synaptic events has little effect on the results (Fig. 3b). These delays results in post synaptic events which are separated in time by a fixed (random) amount between 0 and 5 ms. This suggests that it is the common rhythmic modulation which the neurone is sensitive to rather than the tendency for synchronous inputs. The effect on the output discharge of the paired

neuron model is, however, to restore the tendency for synchronous spikes which have the same common rhythmic modulation as the population of inputs. Thus, although the tendency for synchronous events does not appear to be necessary for the neurone to respond to temporal correlation, the effect within a population of post synaptic neurones is to preserve both aspects of the temporal code. In addition, the strength of correlation within the post synaptic discharges appears to be enhanced, although this may be a feature of the specific parameters in the present simulations. A recent study using a random walk model of cortical neurones found that weakly synchronized inputs did not cause any increase in synchronization in output neurones [7]. Experimental evidence has been presented that input synchrony is an important variable in determining the characteristics of the output discharge of cortical neurones [26].

Similar simulation studies have demonstrated that the presence of weak stochastic correlation can control the bandwidth of the neurone, defined as the frequency components transmitted from pre-to post synaptic discharges, and led to the concept of dynamic modulation of neuronal bandwidth [27]. The present results suggest that this process can also preserve the temporal coding in the correlated spike trains, and further, that the mechanism does not depend on dendritic input location.

The present simulations are designed to model accurately the large degree of convergence in central and peripheral mammalian neural systems [28, 29]. Under conditions of large scale synaptic integration many hundreds of synaptic events contribute to the excitation which generates each output spike [30,31]. In the above simulations there are, on average, 2666 input spikes for each output spike, where each input spike contributes a small increment of excitation to the somatic membrane potential. Studies on the mechanisms underlying neural integration in neurones have proposed that temporal coding in input spike trains will not be preserved under conditions of temporal integration (defined as a large ratio of input to output spikes) [5, 7, 10]. However, as the above simulations demonstrate, the temporal coding carried by each population of 5% of the total synaptic input is transferred to the output discharge of the neurone.

The study of the mechanisms by which spiking neurones encode information in their output discharge, relates to the fundamental questions of how information is represented and processed in the central nervous system [32]. There is currently considerable interest and debate about the underlying mechanisms. Rate coding, coincidence detection and temporal integration have been considered as fundamental mechanisms underlying neural coding [4-10]. Despite the considerable research effort in this area, as yet the basic mechanisms which underlie neural coding are poorly understood [33]. Simulation studies, such as those reported above, are useful tools with which to investigate neural integration. The present simulations have demonstrated that temporal coding, in the form of weak stochastic temporal correlation, can be preserved by spatial temporal integration in passive dendrites. This may be an important mechanism in large scale synaptic integration across different classes of neurone.

## References

1. Singer, W., Gray, C.: Visual feature integration and the temporal correlation hypothesis. *Annual Review of Neuroscience* 18 (1995) 555-586
2. MacKay, W.A.: Synchronized neuronal oscillations and their role in motor processes. *Trends in Cognitive Sciences* 1 (1997) 176-183
3. Riehle, A., Grün, S., Diesmann, M., Aertsen, A.: Spike synchronization and rate modulation differentially involved in motor cortical function. *Science* 278 (1997) 1950-1953
4. Abeles, M.: Role of cortical neuron: Integrator or coincidence detector? *Israel Journal of Medical sciences* 18 (1982) 83-92
5. Shadlen, M.N., Newsome, W.T.: Noise, neural codes and cortical organization. *Current Opinion in Neurobiology* 4 (1994) 569-579
6. Shadlen, M.N., Newsome, W.T.: Is there a signal in the noise? *Current Opinion in Neurobiology* 5 (1995) 248-250
7. Shadlen, M.N., Newsome, W.T.: The variable discharge of cortical neurons: Implications of connectivity, computation and information coding. *Journal of Neuroscience* 18 (1998) 3870-3896
8. Softky, W.R.: Simple versus efficient codes. *Current Opinion in Neurobiology* 5 (1995) 239-247
9. Softky, W.R., Koch, C.: The highly irregular firing of cortical cells is inconsistent with temporal integration of random EPSPs. *The Journal of Neuroscience* 13 (1993) 334-350
10. König, P., Engel, A.K., Singer, W.: Integrator or coincidence detector? The role of the cortical neuron revisited. *Trends in Neurosciences* 19 (1996) 130-137
11. Halliday, D.M.: Generation and characterization of correlated spike trains. *Computers in biology and medicine* 28 (1998) 143-152
12. Cullheim, S, Fleshman, J.W., Glenn, L.L., Burke, R.E.: Membrane area and dendritic structure in type identified triceps surae alpha motoneurons. *Journal of comparative neurology* 255 (1987) 82-96
13. Fleshman, J.R., Segev, I., Burke, R.E.: Electrotonic architecture of type-identified  $\alpha$ -motoneurons in the cat spinal cord. *Journal of Neurophysiology* 60 (1988) 60-85
14. Rall, W., Burke, R.E., Holmes, W.R., Jack, J.J.B., Redman, S.J., Segev, I.: Matching dendritic neuron models to experimental data. *Physiological Reviews* 72 (1992) (Suppl.) S159-S186
15. Segev, I., Fleshman, J.R., Burke, R.E.: Compartmental models of complex neurons. In *Methods in neuronal modeling: From synapses to networks*, eds Koch C, Segev I. (1989) 63-96. MIT Press
16. Jack, J.J.B., Noble, D., Tsien, R. W.: *Electrical Current Flow in Excitable Cells*. 2<sup>nd</sup> Edition Clarendon Press, Oxford (1975)
17. Segev, I., Fleshman, J.R., Burke, R.E.: Computer simulations of group Ia EPSPs using morphologically realistic models of cat a-motoneurons. *Journal of Neurophysiology* 64 (1990) 648-660
18. Cope, T.C., Fetz, E.E., Matsumura, M.: Cross-correlation assessment of synaptic strength of single Ia fibre connections with triceps surae motoneurons in cats. *Journal of Physiology* 390 (1987) 161-188
19. Rinzel, J., Rall, W.: Transient response to a dendritic neuron model for current injected at one branch. *Biophysics* 14 (1974) 759-789
20. Baldissera F., Gustafsson B.: Afterhyperpolarization conductance time course in lumbar motoneurons of the cat. *Acta physiol. scand* 91 (1974) 512-527
21. Moore, G.P., Segundo, J.P., Perkel, D.H., Levitan, H.: Statistical signs of synaptic interaction in neurones. *Biophysical Journal* 10 (1970) 876-900

22. Rosenberg, J.R., Amjad, A.M., Breeze, P., Brillinger, D.R., Halliday, D.M.: The Fourier approach to the identification of functional coupling between neuronal spike trains. *Progress in Biophysics and molecular Biology* 53 (1989) 1-31
23. Halliday, D.M., Rosenberg, J.R., Amjad, A.M., Breeze, P., Conway, B.A., Farmer, S.F.: A framework for the analysis of mixed time series/point process data - Theory and application to the study of physiological tremor, single motor unit discharges and electromyograms. *Progress in Biophysics and molecular Biology* 64 (1995) 237-278
24. Rosenberg, J.R., Halliday, D.M., Breeze, P., Conway, B.A.: Identification of patterns of neuronal activity - partial spectra, partial coherence, and neuronal interactions. *Journal of Neuroscience Methods* 83 (1998) 57-72
25. Calvin, W.H., Stevens, C.F.: Synaptic noise and other sources of randomness in motoneuron interspike intervals. *Journal of Neurophysiology* 31 (1968) 574-587
26. Stevens, C.F., Zador A.M.: Input synchrony and the irregular firing of cortical neurons. *Nature Neuroscience* 1 (1998) 210-217
27. Halliday, D.M.: Weak, stochastic temporal correlation of large scale synaptic input is a major determinant of neuronal bandwidth, *Neural Computation* 12 (2000) 737-747
28. Braitenberg, V., Schüz, A.: *Cortex: Statistics and geometry of neuronal connectivity*. Springer-Verlag, Berlin (1997)
29. Henneman, E., Mendell, L.M.: Functional organization of motoneuron pool and its inputs. In *Handbook of Physiology*. Section 1 Vol 2 Part 1 The nervous system: Motor control (eds Brokxhart, J.M. & Mountcastle, V.B.) American Physiological Society, Bethesda, MD, (1981) 423-507
30. Bernander, Ö., Douglas, R.J., Martin, K.A.C., Koch, C.: Synaptic background activity influences spatiotemporal integration in single pyramidal cells. *Proceedings of the National Academy of Sciences* 88 (1991) 11569-11573
31. Rapp, M., Yarom, Y., Segev, I.: The impact of parallel fiber background activity on the cable properties of cerebellar purkinje cells. *Neural Computation* 4 (1992) 518-533
32. Marr, D.: *Vision*. WH Freeman & Company, San Francisco (1982)
33. Abbott, L. Sejnowski, T.J.(eds): *Neural codes and distributed representations*. MIT Press (1999)